

Supplementary Methods, Tables and Figures

Lin and St. Maurice, “The structure of allophanate hydrolase from *Granulibacter bethesdensis* provides insights into substrate specificity in the amidase signature family”

Supplementary Methods

Cloning, expression and co-purification of P. syringae AH and UC. Genomic DNA from *Pseudomonas syringae* pv. *tomato* str. DC3000 (ATCC No. BAA-871D-5) was obtained from American Type Culture Collection (Manassas, VA). The urea carboxylase gene (GenBank: ZP_07230257.1) was amplified using primers (5'- ATT TGC TAG CTT CGA CAA ACT GCT GAT CGC CAA CCG T -3') and (5'- GAT CGT CGA CTT ATC AGT CTG CTG CCA GCA CTA CGA C -3'). The PCR-amplified fragment was digested with *NheI/SalI* and ligated into the *NheI/SalI* digested pET28a-(His)₈-TEV vector, downstream of the T7 promoter, N-terminal (His)₈ tag and rTEV protease recognition sequence (1). The *P. syringae* allophanate hydrolase gene (GenBank: NP_794005) was amplified using primers (5'- ATG CCC TGC AGG CGA ACG ACA CAG CTC TGC CGA AC -3') and (5'- ATG TGC TAG CTT ATC ACA GCT GTT GCA GGT AGG C -3'). The PCR amplified fragment was digested with *SbfI/NheI* and ligated into the *PstI/NheI* digested pET28a-(His)₈-TEV vector, downstream of the T7 promoter, N-terminal (His)₈ tag and rTEV protease recognition sequence.

Non (His)₈-tagged *PsUC* and *PsAH* was cloned using pET28a-(His)₈-TEV-*PsUC* and pET28a-(His)₈-TEV-*PsAH*. A second *NcoI* restriction site was introduced downstream of the coding sequence for the (His)₈ tag, such that the (His)₈ tag coding sequence was bracketed by two *NcoI* restriction sites. The CTAGTG was mutated into an *NcoI* site (CCATGG) by QuikChange site-directed mutagenesis (La Jolla, CA 92037) using Pfu Turbo polymerase. The vectors were subsequently digested with

NcoI, gel purified and re-ligated. The sequences of the constructed vectors were verified by Functional Biosciences (Madison, WI).

All proteins were expressed in *E. coli* BL21(DE3) cells. For expression of *PsAH*, the cells were transformed with the pET28a-(His)₈-TEV plasmid encoding (His)₈-tagged or non-(His)₈-tagged *PsAH* and were grown in LB media containing 25 µg/mL kanamycin. For expression of *PsUC*, the cells were co-transformed with pCY216-BirA (1) and (His)₈-tagged or non-(His)₈ tagged *PsUC*, and grown in LB media containing 25 µg/mL kanamycin and 100 µg/mL spectinomycin, to facilitate *in vivo* biotinylation of *PsUC*. LB media (5 mL) was inoculated with a single colony transformant and incubated overnight at 37°C. The overnight culture was used to inoculate 50 mL of LB media to an OD₆₀₀= 0.2, which was grown at 37°C to an OD₆₀₀ = 0.8. The cultures were chilled in an ice water bath prior to induction with IPTG to a final concentration of 1 mM. The cultures were transferred to a 16°C shaking incubator for 24 h prior to cell harvesting.

Ni²⁺-affinity chromatography was used for co-purification studies. The harvested cells expressing either (His)₈-tagged *PsAH* (His-*PsAH*), (His)₈-tagged *PsUC* (His-*PsUC*), non-(His)₈-tagged *PsAH* (*PsAH*) or non-(His)₈-tagged *PsUC* (*PsUC*) were disrupted by sonication in buffer containing 50 mM HEPES (pH 8.0), 300 mM NaCl and were centrifuged at 12000 rpm, 4°C. The supernatant from each set of cells was removed and these supernatants were mixed in the following combinations: His-*PsAH*/*PsUC*, His-*PsUC*/*PsAH*, *PsAH*/*PsUC*, His-*PsAH*/His-*PsUC*. The mixed supernatants were incubated on a rocker for 30 min at 4°C. The supernatants were loaded onto a mini-spin column containing 100 µL Ni²⁺-Profinity IMAC resin. The enzyme was washed using buffer containing 20 mM imidazole and eluted from the column using buffer containing 300 mM imidazole. The load and

eluted protein samples were analyzed by sodium dodecyl sulfate-polyacrylamide gel electrophoresis (SDS-PAGE).

Table S1. Results from analysis of the *GbAH* structure using the DALI server.

Enzyme ¹	PDB ID	Z score	r.m.s.d	Sequence identity (%)
GatA	3h0m	51.3	2.0	28
Probable amidase	2dc0	49.4	2.1	32
MAE2	1ock	44.9	2.5	28
NylA	3a2q	41.6	2.6	26
PAM	1m21	41.5	2.5	15
FAAH	1mt5	35.6	2.9	8.9

¹ GatA: *Aquifex aeolicus* GatA; Probable amidase from *Thermus thermophilus*; MAE2: *Bradyrhizobium japonicum* Malonamidase E2; NylA: *Arthrobacter sp.* 6-aminohexanoate cyclic dimer hydrolase; PAM: *Stenotrophomonas maltophilia* peptide amidase; FAAH, *Rattus norvegicus* fatty-acid amide hydrolase.

Figure S1. Dimerization interfaces of GbAH.

(A) Table of dimerization interface analysis for GbAH, *B. japonicum* malonamidase (PDB ID: 1OCL) and rat fatty acid amide hydrolase (PDB ID: 1MT5). Calculated by the PDBe PISA server. (B) Stereo figure showing the alignments of the 3 predicted dimerization interfaces of GbAH, with malonamidase (PDB ID: 1OCL) and fatty acid amide hydrolase (PDB ID: 1MT5). Interface 1 is colored cyan, interface 2 is colored orange, and interface 3 is colored green. Fatty acid amide hydrolase and malonamidase are colored magenta and grey, respectively, with the corresponding chains in the second subunit colored in light cyan, light magenta and light grey.

Figure S2. Chemical structures of substrates and substrate analogues used in the present study.

Figure S3. Representative initial velocity vs. [substrate] plots for GbAH Tyr₂₉₉ and Arg₃₀₇ mutants with allophanate and substrate analogs using the phenol hypochlorite assay.

The data was fitted to the Michaelis-Menten equation for single-enzyme systems. The k_{cat}/K_m are estimated from the slope of the regression line for v_i vs. substrate concentration at low substrate concentration (i.e. $[S] \ll K_m$). The insets display representative raw data for [ammonia] vs. time at varying initial concentrations of allophanate or substrate analogs. (a)~(c) Activity of GbAH Tyr₂₉₉/Arg₃₀₇ double mutants with allophanate. (d)~(k) activity of GbAH wt and Tyr₂₉₉, Arg₃₀₇ single mutants with biuret or malonamide. Note: this figure extends across two pages.

Figure S4. Size exclusion chromatography of wild-type and site-directed mutants of GbAH.

Representative chromatograms for wild-type GbAH (GbAH wt) and site-directed mutants. The peak at elution volume of 15 mL corresponds to the predicted molecular weight for the wild-type GbAH dimer (MW = 130kDa). The elution profiles for Tyr₂₉₉ and Arg₃₀₇ mutants match that of the wild-type enzyme. The peak at an elution volume of 15.5 mL corresponds to the dimer for the GbAH C-terminal deletion mutant (MW = 100kDa). The column was calibrated with molecular weight standards as previously described (1).

Figure S5. The position of the specificity loop in GbAH compared to malonamidase.

Stereo figure showing the alignment of GbAH and *B. japonicum* malonamidase (PDB ID: 1OCL) active sites. AH carbon atoms are colored in cyan and malonamidase carbon atoms are colored in white. The active site residues and bound malonate are represented as CPK-colored sticks. The specificity loop in each enzyme is presented in cartoon format. The clashes that would arise between the AH specificity loop and malonamidase side chains and substrates are measured and labeled in black.

Figure S6. The ammonia tunnel is present in GbAH.

(A) Overall structure alignment of a GbAH monomer with *Staphylococcus aureus* GatCAB (PDB ID: 2F2A). Tunnels in GbAH are calculated using CAVER (2, 3). AH is colored cyan, GatA is colored in pink, GatB is colored brown and GatC is colored purple. The two tunnels in GbAH are displayed as transparent surfaces. The substrate enters the active site through the yellow-colored tunnel, and ammonia may be

released through the grey-colored tunnel. **(B)** A magnified view of the *GbAH* active site, showing the accessibility of the two tunnel entrance sites.

Figure S7. Urea carboxylase and allophanate hydrolase do not associate *in vitro*.

(A) Representative chromatograms from size exclusion chromatography of *Pseudomonas syringae* allophanate hydrolase (*PsAH*), *P. syringae* urea carboxylase (*PsUC*) and *PsAH/PsUC* together. The peak at an elution volume of 15 mL corresponds to the predicted molecular weight for the wild-type *PsAH* dimer (MW = 130kDa), and the *PsUC* monomer (MW=140 kDa). Co-application of both *PsAH* and *PsUC* on the size exclusion column does not alter the elution profile, indicating that a stable complex is not formed between *PsAH* and *PsUC*. The column was calibrated with molecular weight standards as previously described (1). **(B)** SDS-PAGE gel showing *PsUC* and *PsAH* do not co-purify *in vitro*. Purified protein prior to and after Ni²⁺ purification was resolved on SDS-PAGE gel. Protein sample loaded onto Ni²⁺ column, prior to purification, and the protein eluted from the column are shown on the gel. Each lane is corresponding to His-tagged UC or AH, non His-tagged UC or AH, and co-purified proteins, illustrated as above the gel.

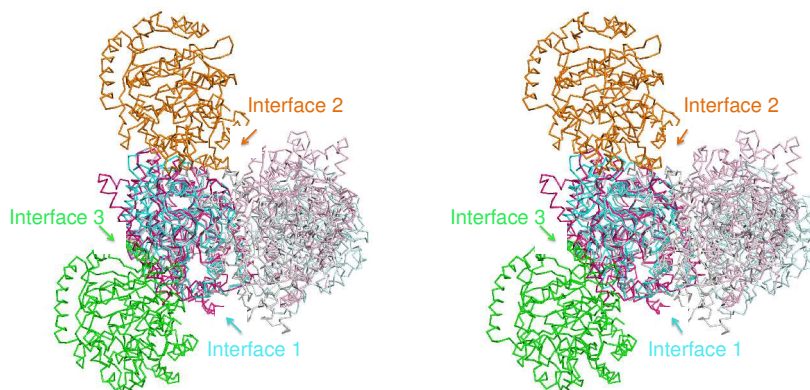
References:

- (1) Lietzan, A. D., Menefee, A. L., Zeczycki, T. N., Kumar, S., Attwood, P. V., Wallace, J. C., Cleland, W. W., and St Maurice, M. (2011) "Interaction between the Biotin Carboxyl Carrier Domain and the Biotin Carboxylase Domain in Pyruvate Carboxylase from *Rhizobium etli*." *Biochemistry* 50, 9708-9723.
- (2) Petrek, M., Otyepka, M., Banas, P., Kosinova, P., Koca, J., and Damborsky, J. (2006) CAVER: a new tool to explore routes from protein clefts, pockets and cavities. *BMC Bioinformatics* 7, 316.
- (3) Damborsky, J., Petrek, M., Banas, P., and Otyepka, M. (2007) Identification of tunnels in proteins, nucleic acids, inorganic materials and molecular ensembles. *Biotechnol. J.* 2, 62–67.

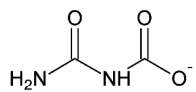
A.

	Interface	Interface area (Å ²)	ΔG (kcal)
AH	1	1092.9	-13.7
	2	812.1	-7.3
	3	792.4	-4.8
MAE2	1	1493.1	-6.8
	2	445.1	4.0
FAAH	1	1607.0	-18.5
	2	385	-4.5

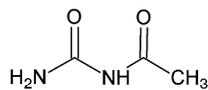
B.



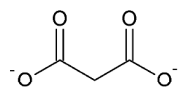
Lin and St. Maurice; **Figure S1**



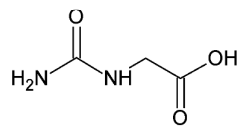
allophanate



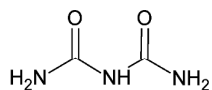
acetyl-urea



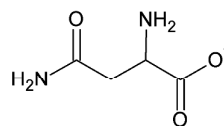
malonate



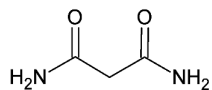
hydantoic acid



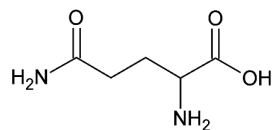
biuret



asparagine

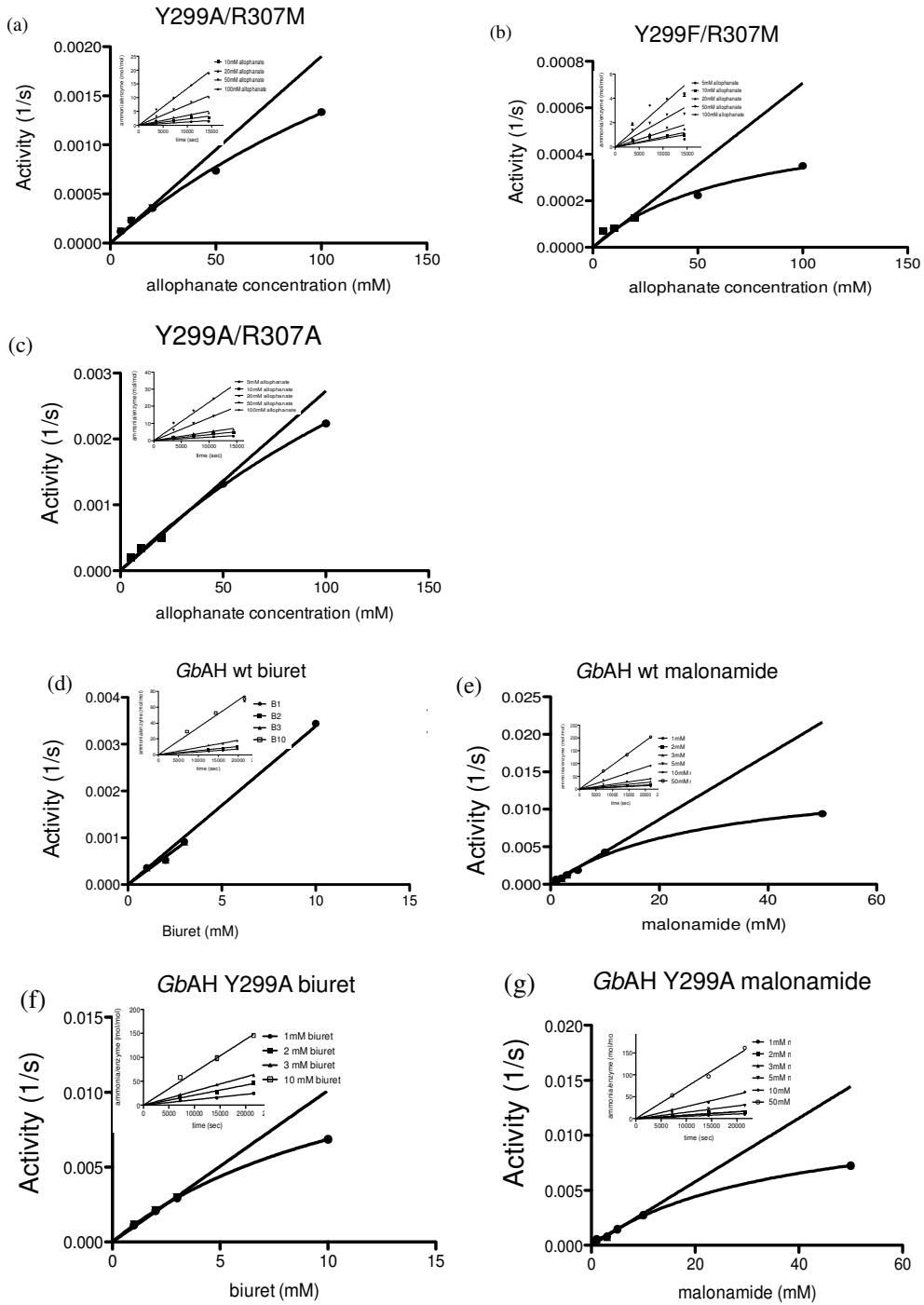


malonamide

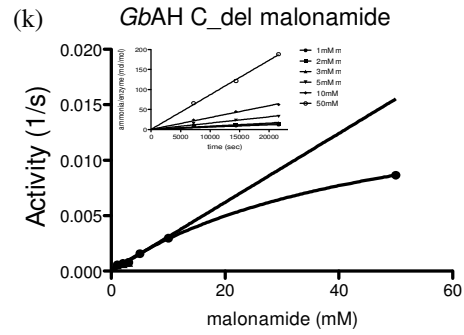
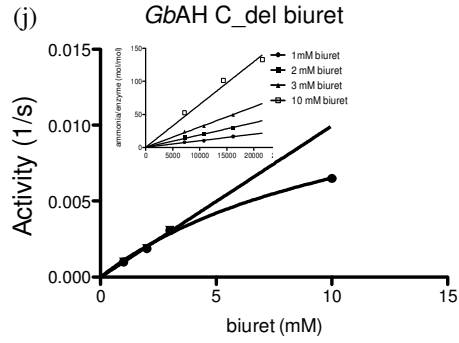
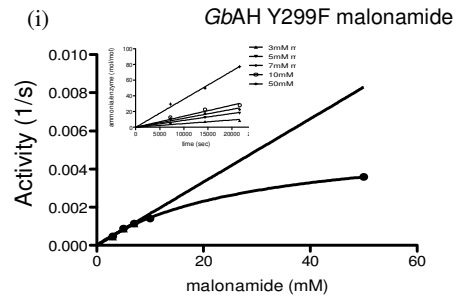
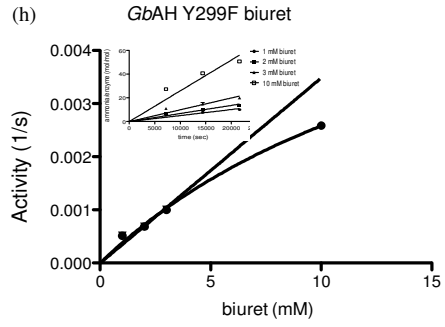


glutamine

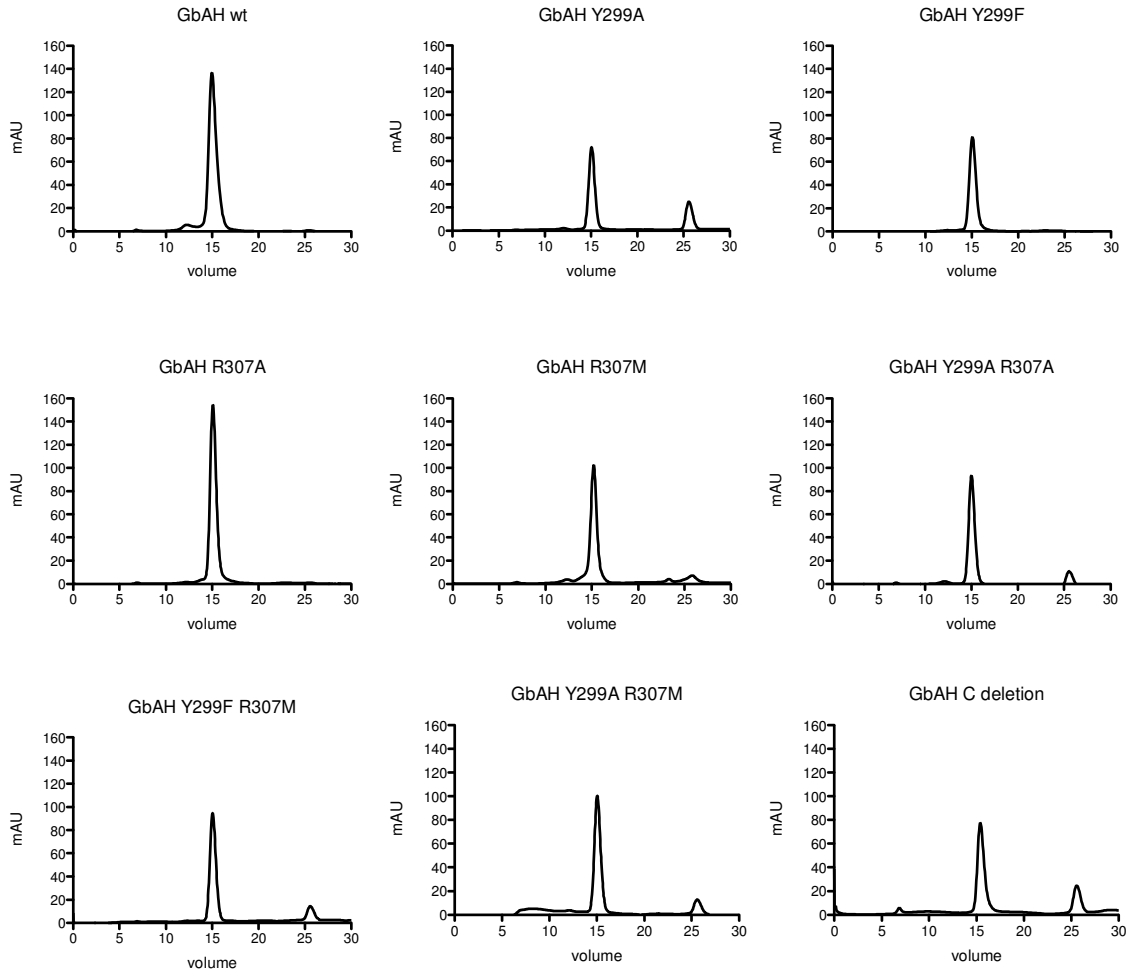
Lin and St. Maurice; **Figure S2**



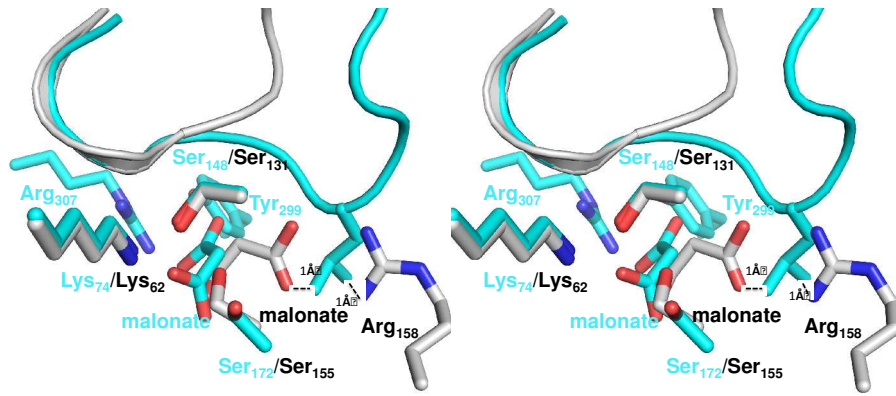
Lin and St. Maurice; Figure S3 (Part 1)



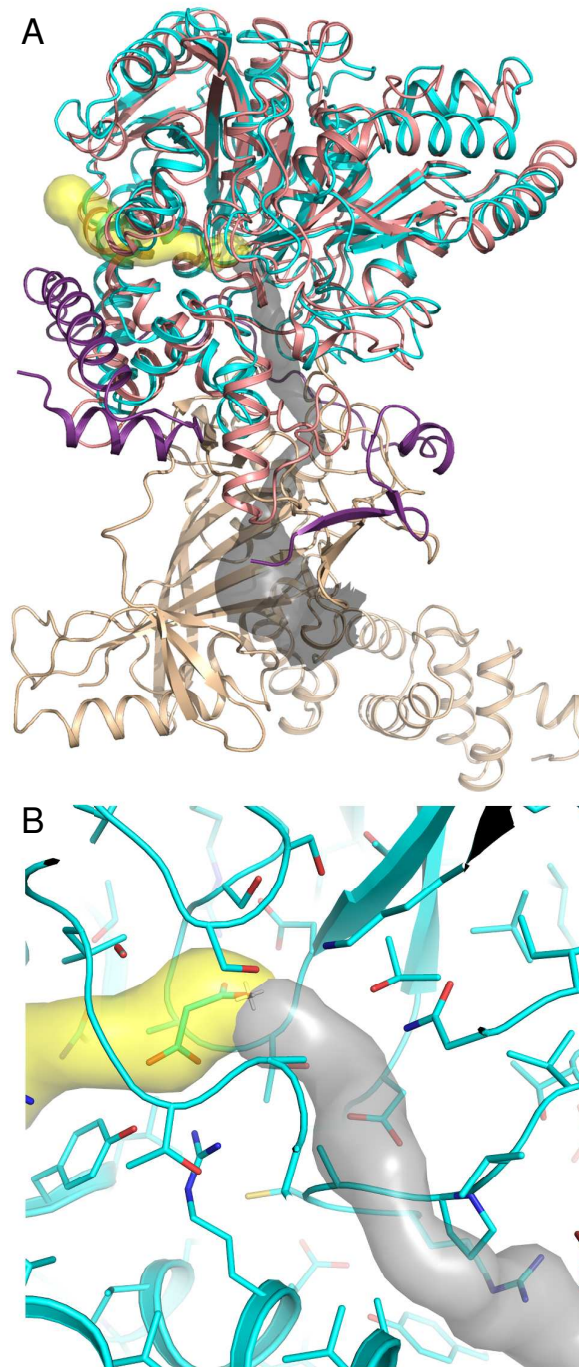
Lin and St. Maurice; **Figure S3 (Continued)**



Lin and St. Maurice; **Figure S4**

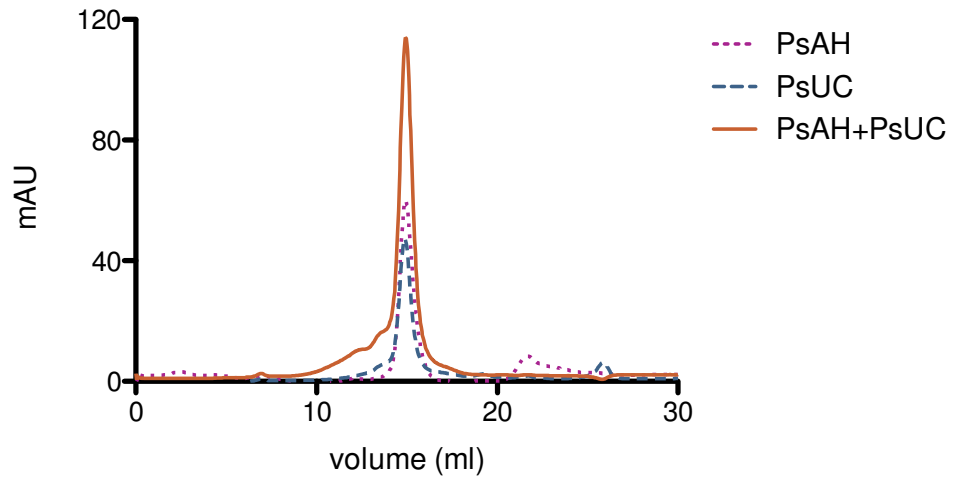


Lin and St. Maurice; **Figure S5**

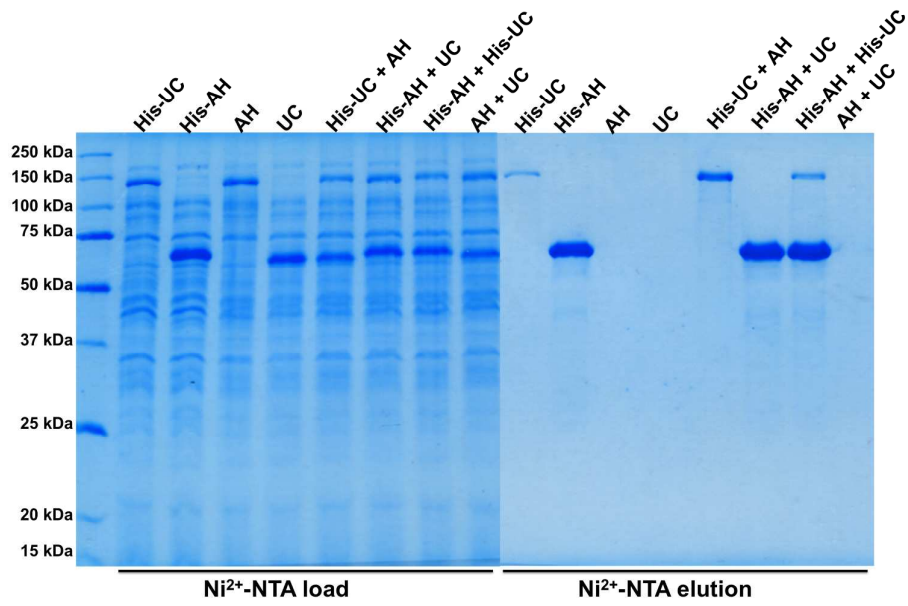


Lin and St. Maurice; **Figure S6**

A.



B.



Lin and St. Maurice; **Figure S7**